Chapter 1
Ellipsometry: A Survey of Concept

Christoph Cobet

Abstract Already the first attempts by Paul Drude in the late 19th century demonstrate the abilities of optical polarimetric methods to determine dielectric properties of thin layers. Meanwhile ellipsometry is a well-established method for thin film analysis. It provides material parameters like n and k even for arbitrary anisotropic layers, film thicknesses in the range down to a few Ångström, and ellipsometry is used to analyze the shape of nm-scale surface structures. But, the determination of such manifold information by means of light polarization changing upon reflection at a sample surface requires appropriate optical models. This introductory chapter will provide a general overview and explanation of theoretical and experimental concepts and their limitations. It will introduce the very basic data evaluation steps in a comprehensive manner and will highlight the principal requirements for the characterization of functional organic surfaces and films.

1.1 Classification

Ellipsometry and other types of polarimetry are well known optical methods which are used since more then 100 years for analytic purposes. Here, the term ellipsometry is certainly linked to the polarization sensitive optical investigation of planar solid state structures (metals, semiconductors) with polarized light. Optical methods in general benefit from the fact that they are usually non destructive and applicable in various environments. The object under investigation can be stored in vacuum, gas, liquid, and even in solid ambiances as long as the surrounding material is transparent within the spectral range of interest. By taking advantage of the polarizability of light, it is possible to measure for example thin film properties like the refractive index and the thickness with very high accuracy and without the need of a reference. Because of these abilities ellipsometry is meanwhile a very popular method used in many different application fields. Accordingly, a couple of books, book chapters,

C. Cobet (✉)
Center for Surface- and Nanoanalytics, Johannes Kepler Universität Linz, Altenbergerstrasse 69, 4040 Linz, Austria
e-mail: christoph.cobet@jku.at

K. Hinrichs, K.-J. Eichhorn (eds.), *Ellipsometry of Functional Organic Surfaces and Films*, Springer Series in Surface Sciences 52, DOI 10.1007/978-3-642-40128-2_1,

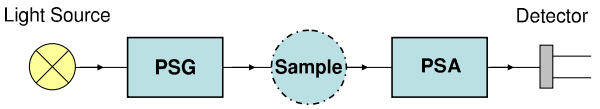

Fig. 1.1 Principle concept of ellipsometric and polarimetric techniques. The Polarization State Generator (PSG) and Polarization State Analyzer (PSA) may consist of a polarizer or a combination of a polarizer and retardation component

and review articles provide already comprehensive information about the method ellipsometry itself and the physical/mathematical background especially for thin film applications [1–7]. Therefore, it is not the intention to repeat here once again all technical details. We would rather like to provide in this chapter an overview about relevant aspects which are needed to empathize the analytical possibilities concerning functional organic surfaces and films. Furthermore, we will address limitations of the method and the underlying physical models.

The common concept behind the methods ellipsometry and polarimetry rests upon the analysis of a polarization change of light which is interacting with the object of interest. Here, we follow one of the definitions given by Azzam [8] in 1976 which was discussed in connection to the 3rd International Conference on Ellipsometry. Accordingly "An ellipsometer (polarimeter) is any instrument in which a TEEMW—transverse electric electromagnetic wave—generated by a suitable source is polarized in a known state, interacts with a sample under investigation, and the ellipse (the state of polarization) of the radiation leaving the sample is analyzed". This concept implies that both the polarization state of the light before and after interaction with the sample can be modified or determined (Fig. 1.1). Investigations for example of atmospheric and extraterrestrial phenomena where the polarization properties of the light source itself are analyzed or where the light polarization before interacting with the object of interest is not accessible are not considered in this definition [9]. Furthermore, only linear optical effects are considered and phenomena, where the light frequency is changed like in Raman scattering, second harmonic generation and sum frequency processes, are excluded.

With the definition above, ellipsometry can be used to analyze reflected, transmitted, scattered, and diffracted light (Fig. 1.2). Ellipsometric transmission measurements are so far preferentially used to analyze birefringence, optical activity, circular birefringence, and in case of a small absorption also circular dichroism. In this book the discussion is focused on the analysis of organic surfaces and stratified films in reflection type measurements. Thus, the sample is illuminated under an oblique angle of incidence and the specular reflection is analyzed (Fig. 1.2(a)). Accordingly, all presented theoretical models assume that the analysis takes place in the optical far field where the approximation of plane waves is reasonable i.e. the distance between analyzer/detector and the sample has to be much larger than the wavelength and possible lateral inhomogeneities of the sample.

The applied optical models assume furthermore monochromatic or quasi-monochromatic electromagnetic waves which are reflected at the sample by retaining total polarization of the incident light. The electromagnetic wave before and

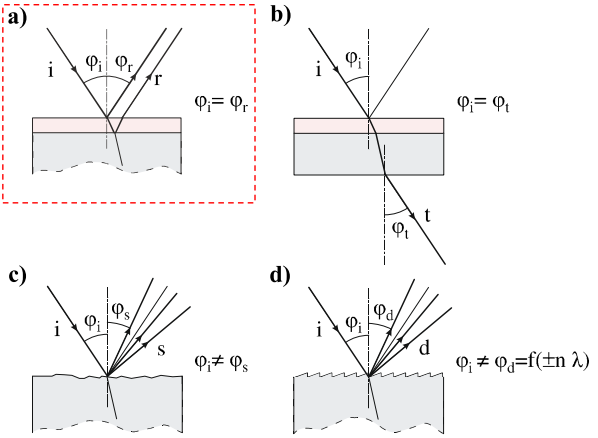

Fig. 1.2 Fundamental interaction of light which incidents on different samples under an angle φ_i: (**a**) reflection, (**b**) transmission, (**c**) scattering, and (**d**) diffraction. All introduced ellipsometric problems are reflection measurements (*red dashed box*)

after reflection is completely defined by an unique elliptical polarization state which gives the method the name "ellipsometry".

The term "polarimetry", in contrast, is usually used in a more general context including the analysis of non-specular reflected or scattered light from inhomogeneous samples or surfaces (Fig. 1.2(b–d)). In this context polarimetry is often used as a contact free method in order to determine morphology aspects [10]. Strongly related to scattering processes is a partial depolarization of the light. As we will discuss later, this requires extended optical models. A strict delimitation between ellipsometry and polarimetry, however, is neither possible nor helpful. In reality both terms are used with much overlap and a number of specific approaches are used by related proper names (Sect. 1.5.6).

Bearing in mind that the fundamental electromagnetic theory remains the same for all different regions of the spectrum, it is also not surprising that methods like polarimetry and ellipsometry are applied in much the same way from the region of radio frequencies over the infrared, visible and ultra violet to the X-/γ-ray spectral range. But due to experimental peculiarities, the knowledge transfer between the communities is unfortunately low. This book will bridge in parts this spacings by including all sections of the "optical" spectral range which includes here the infrared, the visible, and the ultraviolet wavelength/frequency range. Nevertheless, it could be particularly beneficial to consider also applications in the radio, radar, and microwave region. Related to the longer wavelength, the determination of structural and morphological properties in this range is historically stronger in the focus. Respective theoretical models for the data processing are therefore rather sophisticated and can be adapted for the optical spectral range [9, 11].

1.2 Historical Context

In a historical review the first observations of the polarization properties of light is directly linked to the discovery that light changes its polarization state after reflec-

tion on, for example, glass windows of buildings and is associated with names like Etienne-Louis Malus, David Brewster, and Augustin-Jean Fresnel. In the 1800's the polarization change of reflected light was used in a couple of works to study the optical properties of metals. A first description of elliptically polarized light attributes to Jamin [12–14]. He has observed this polarization after reflection of linearly polarized light on metal surfaces which were decorated with transparent overlayers. It turned out, that the elliptical polarization is the most arbitrary polarization state whose constituting parameters have to be determined when planar homogeneous layers are investigated.[1] For this reason, the name "ellipsometry" was established by Rothen [15] almost 100 years later in 1945 for such kind of measurements. However, a first comprehensive description of the method as a technique to study the optical properties of thin films was given already by Paul Drude in the late 19th century. He was measuring the optical properties of metals under consideration of unintentional and intentional overlayers. Furthermore, he could model the measured polarization changes by an extension/modification of Fresnel's equation, which are originally made for the reflection of light on a single planar interfaces, to the problem of two stacked interfaces [16–18]. With this approach it was possible to determine bulk and film dielectric properties as well as film thicknesses.

70 years later these analytical potentials attract a lot of attention in connection with the invention and development of semiconductor electronics. The investigation of SiO_2 films on Si is probably one of the best examples for the abilities of the method until now. On the other hand, the progress in semiconductor electronics considerably accelerates the development of computers and the automation possibilities. With the help of microprocessors it was now possible to build automatic spectroscopic ellipsometers (SE) which made the method much more attractive for a wider community. Large steps forward in development and improvement are associated to the work of Aspnes [19]. This progress also lead to more advanced applications and setups with an appropriate spectral range and a reasonable resolution. In the following different angles of incidence or different polarization states of the incident light were used in order to extract more accurate information from rather complex samples. Meanwhile multi-layer structures, all kinds of optical anisotropy, magneto-optical effects, as well as 3D inhomogeneous structures are accessible. But the final breakthrough for the method is definitely linked to the availability of easy-to-use analysis software packages. Hence, it became possible to extract useful information even for complicated sample structures with moderate efforts. In this context it is also apparent why the optical characterization of organic films, which are often anisotropic and inhomogeneous, was mostly restricted to reflection and transmission measurements for a long time. The wide spread developments in the recent years are documented for example in the proceedings of the conference series "International Conferences on Spectroscopic Ellipsometry" [20–24]. Concerning the newer developments we would also refer to a number of publications which provide further details [8, 25–29].

[1] Possible contributions of unpolarized light are ignored here.

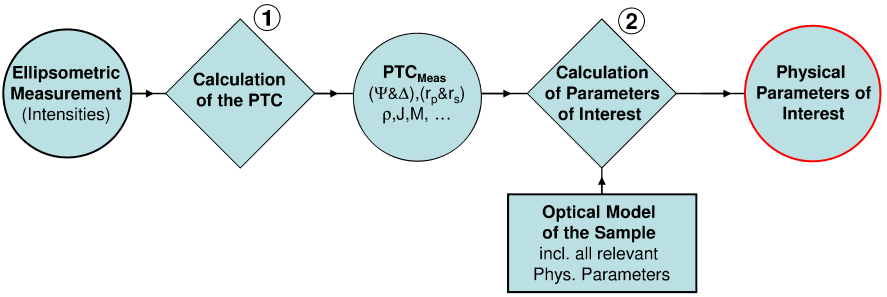

Fig. 1.3 Basic data evaluation steps in an ellipsometric measurement. The *left hand side* of the flow chart depicts the determination of the polarizing properties of the sample which are represented e.g. by the ellipsometric angles Ψ and Δ or in more general by polarization transformation coefficients (PTC). In the *right hand part* these polarization parameters are translated in physical sample parameters with the help of a qualitative sample model

1.3 Measurement Principles

1.3.1 Data Recording and Evaluation Steps

As it was mentioned, ellipsometry in principal determines polarization changes upon interaction with a sample. Subsequently it is possible to extract, for instance, layer thicknesses or dielectric properties in a "reference free" manner. Thus, two major data evaluation steps are needed in ellipsometry in order to receive information about the sample (Fig. 1.3). In parts they depend on each other. Nevertheless it is helpful to divide the problem in such basic steps and it seems worthwhile to discuss these steps briefly to obtain a general understanding of the method.

All kinds of ellipsometers are primary measuring intensities with light sensitive detectors. These intensities have to be related in the first evaluation step to the polarization change induced by the sample (left hand part of Fig. 1.1). Therefore, each ellipsometer is recording the intensity with different incident light polarizations or analyzer orientations in order to obtain relative intensities. With an appropriate set of such arrangements one can deduce out of it, how the sample under investigation changes an arbitrary polarization of the incident light. It is evident that a respective theoretical formalism is needed which translates the detector signals to the polarization properties of the sample. As it will be discussed later, the probability of the sample to change the polarization of monochromatic light can be described for an isotropic sample, if no depolarization takes place, by two parameters. Quite often the so-called ellipsometric angles Ψ and Δ are used. In case of anisotropic structures up to 6 parameters are needed. According to reference [8] these parameters are denoted here as "polarization transformation coefficients" (PTC). If depolarization effects are apparent, the number of parameters increases even further. For the moment it is important to note that the PTC's depend on the angle of incidence, the wavelength, and probably on the sample orientation, too.

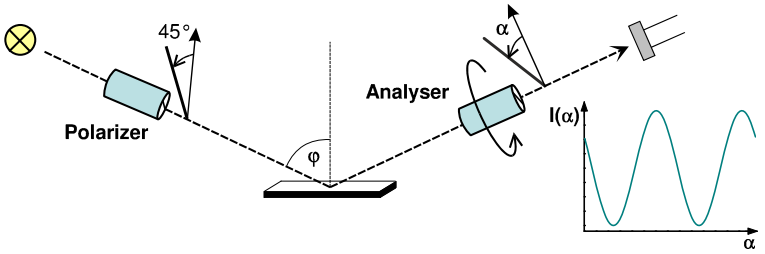

Fig. 1.4 Principal of a rotating analyzer ellipsometer. The polarizer is here fixed with the transmission axis tilted by 45° with respect to the plane of incidence. The intensity signal recorded at the detector for a certain wavelength by rotating the analyzer is of a sinusoidal form with a periodicity of 2α

A very common and simple ellipsometer is the so-called rotating analyzer ellipsometer. It's principle arrangement and the signal recorded at the detector by rotating the analyzer is shown in Fig. 1.4 (q.v. Sect. 1.5). With at least three different analyzer positions it is possible to assign the sinusoidal dependence of the intensity as a function of the rotation angle α by means of the two $\sin(2\alpha)$ and $\cos(2\alpha)$ Fourier-coefficients s_2 and c_2, respectively. With the later briefly explained mathematical formalism it is possible to calculate Ψ and Δ of an isotropic non-depolarizing sample according to

$$\tan\Psi = \sqrt{\frac{1+c_2}{1-c_2}}, \qquad \cos\Delta = \frac{s_2}{\sqrt{1-c_2^2}}. \tag{1.1}$$

In a second step the information about the polarization change by the sample (the PTC's or Ψ and Δ) should be translated in to intrinsic sample properties which are not anymore related to a certain measurement configuration (right hand part in Fig. 1.3). Such intrinsic sample properties are, for instance, layer dielectric functions, layer thicknesses, or volume fractions in inhomogeneous media.

In order to calculate intrinsic properties from the PTC's again, an adequate theoretical description is required. This means that the reflection process depicted in Fig. 1.2(a) has to be specified in more detail. In the very simple and ideal case of a planar abrupt surface of a infinitely thick isotropic sample this connection is given by the well known Fresnel equation. The hereby defined reflection coefficients r_p and r_s for light polarizations parallel and perpendicular to the plane of incidence determine the ellipsometric angles Ψ and Δ:

$$\frac{r_p}{r_s} = \tan\Psi e^{i\Delta}. \tag{1.2}$$

Light reflection from the backside of the sample is neglected in this model. For stratified anisotropic media optical layer models are used in order to calculate the respective PTC's for a given sample structure. In many cases, it is nevertheless possible to define generalized Fresnel equations. The sample parameters are usually

obtained by a fit routine comparing the measured PTC's with respective PTC's calculated from the applied optical model.

At this point it is already obvious that the number of parameters which can be deduced is limited. By measuring Ψ and Δ in a single wavelength measurement at one angle of incidence and sample orientation, ellipsometry can provide two intrinsic sample parameters. Therefore, it has to be ensured that there is a reasonable sensibility to the parameter of interest. In highly absorbing materials it can happen for instance that the penetration depth of light is so small that the electric field in the layer of interest is already damped too strongly. In anisotropic samples the special case might occur in which the electric field vector of the refracted light inside the sample is almost perpendicular to the optical axis of interest. In both examples the sensibility could be low. By using commercially available fit routines, such problems can be tested by means of the so-called standard error. Finally, it has to be ensured that the parameters of interest are not coupled to each other which happens if both of them change the polarization properties of the sample in the same manner. For example, it is sometimes difficult to measure a layer thickness and it's refractive index independently from each other. In a numerical fit, the parameter coupling can be tested by means of the covariance matrix of the standard errors.

The discussion of restrictions in the second evaluation step should emphasize that qualitative information about the sample structure are essential in order to obtain good quantitative results. Indications for deficiencies in the assumed sample structure are for example unexpected interference signatures or an inconsistent dispersion of a deduced dielectric function.

The simple scheme of Fig. 1.3 does not include the important and sometimes demanding step of the definition of appropriate measurement geometries (angle of incidence, sample orientation, etc.) in order to achieve the best possible sensitivity to the sample parameters of interest. It is often not worthwhile to measure just in all possible configurations (e.g. in the whole accessible angle of incidence range). Configurations with low sensitivity to the parameter of interest (e.g. very high or low angles of incidence) may just increase the error in the final result. Appropriate configuration can be chosen by some simple preliminary considerations. If necessary, these can be subsequently modified in an iterative procedure. Thin films are usually best measured at incidence angles near the Brewster angle of the respective substrate material. In some cases it is more efficient to calculate the best configuration in a preliminary simulation.

Since all other evaluation steps are based on the chosen measurement configurations a final flow chart of an ellipsometric measurement may appear rather complicated (Fig. 1.5). In this resulting scheme the significance of an appropriate optical model becomes again evident. It is important to remember that ellipsometry is initially reference free measuring how a sample changes the polarization of an incident light beam. All subsequently derived parameters depend on the best possible assumption of the sample structure and the validity of the applied optical models. Following Eugene A. Irene, who has brought this into phrase, this means in turn that if the information about the sample structure is insufficient: "Ellipsometry is perhaps the most surface sensitive technique in the universe. However you often don't know what it is you have measured so sensitively".

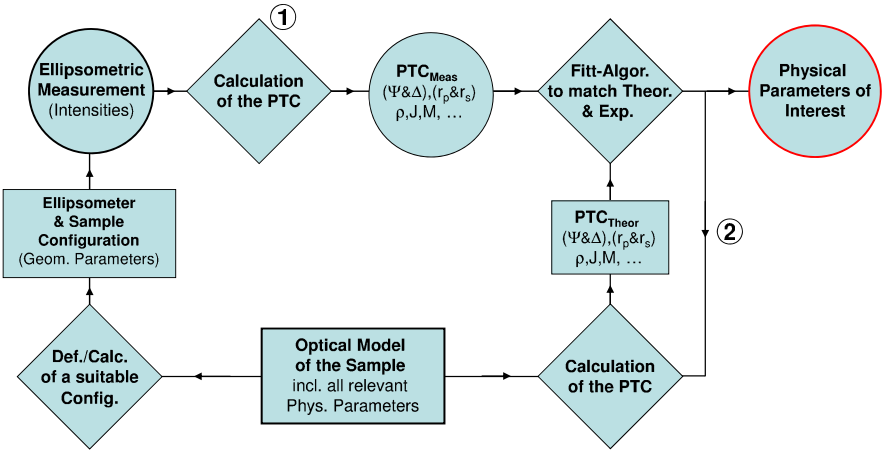

Fig. 1.5 Extended scheme of the data evaluation in an ellipsometric measurement. The two major calculation steps, which can be found already in the simplified representation of Fig. 1.3 are labeled ① and ②

1.3.2 Determination of Ψ and Δ

The determination of Ψ and Δ or the more generalized PTC's of a sample requires some mathematical tools (calculation step ① in Figs. 1.3 and 1.5). First of all a suitable description of polarized light is needed. Furthermore, all optical components including the sample under investigation have to be represented according to their ability to change the state of polarization. These theoretical tools can be finally used to calculate relative intensities which are measured at a detector or, in turn, to determine the PTC's of the sample from the measured intensities.

1.3.2.1 Polarized Light

To simplify the problem as much as possible, assumptions concerning the propagation of light between optical components and the sample are necessary.

- Since linear optical effects are investigated each wavelength λ is addressed separately in a quasi-monochromatic approximation.
- The distances between the optical components are much larger than the wavelength and the coherence length of the light. We can assume planar transversal electromagnetic (TEM) waves propagating only in forward direction from the light source to the detector. In other words, all optical components interact independently, one after another, with the light and interferences between them are avoided. This assumption has to be critical reviewed, e.g. for laser light sources where the coherence length is much larger than for conventional light sources and in near field experiments.

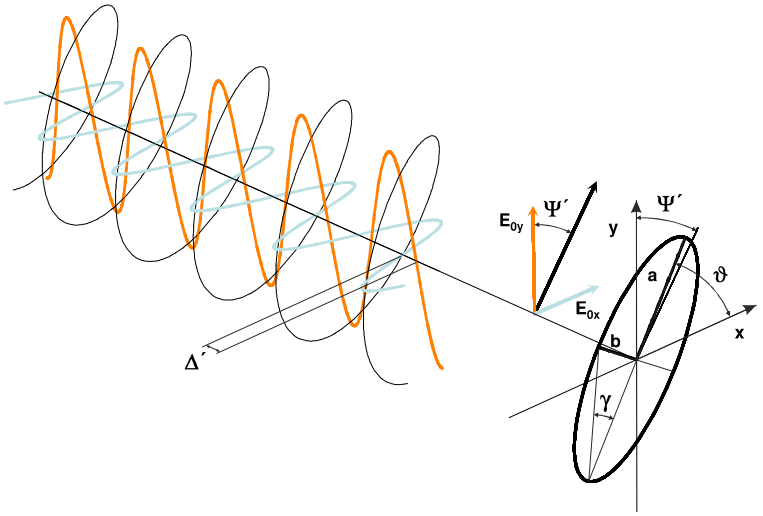

Fig. 1.6 Elliptically polarized light and the projected polarization ellipse. Mathematically the polarization state is defined by three equivalent parameter sets [Ψ'/Δ'—amplitude quotient and phase difference], [ϑ/γ—azimuth angle and ellipticity], and $\chi = 1/\tan\Psi \exp[i\,\Delta]$

- The surrounding medium is assumed isotropic and homogeneous (air, vacuum, water, etc.). Thereby the polarization state does not depend on the propagation direction and can be separately considered.
- The magnetic susceptibility is constantly one in all optical experiments and the polarization of light is fully described by the electric fields.

For the mathematical description of a polarization one can choose without further loss of generality a Cartesian coordinate system so that the light propagates along the positive direction of the z-axis. A common description of an arbitrarily planar monochromatic TEM wave is then given by

$$\begin{aligned} E_x &= E_{0x} \exp\big[i(kz - \omega t)\big] \exp[i\delta_x], \\ E_y &= E_{0y} \exp\big[i(kz - \omega t)\big] \exp[i\delta_y]. \end{aligned} \tag{1.3}$$

Equation (1.3) represents the general case of an elliptical polarization as illustrated in Fig. 1.6. The wave vector $k = 2\pi/\lambda$ and the angular frequency $\omega = 2\pi\nu$ are connected by the known dispersion relation for TEM waves in transparent media. The orientation of the two perpendicular basis vectors in x- and y-direction is free of choice for the moment. The amplitudes E_{0x} and E_{0y} together with the phases δ_x and δ_y for the x and y component, respectively, define the polarization of the light. This set of information can be merged in a so-called Jones vector [30]:

$$\bar{E}^{Jones} = \begin{pmatrix} E_{0x} \exp[i\delta_x] \\ E_{0y} \exp[i\delta_y] \end{pmatrix}. \tag{1.4}$$

However, the absolute phase is not measurable and the absolute intensity ($I \sim E_{0x}^2 + E_{0y}^2$) is an arbitrary value which is not of interest in an ellipsometric measurement. The polarization state is therefore already fully defined by only two parameters: The relative amplitude $\tan \Psi' = E_{0x}/E_{0y}$ and phase $\Delta' = \delta_x - \delta_y$ of the x and y component. Sometimes these two parameters are combined in a single complex number $\chi = 1/\tan \Psi' \exp[i\Delta']$. Another alternative representation refers to the ellipse, which yields from a projection of the electric field vector to the x–y-plane. The respective parameter pair is given by the azimuth angle ϑ between the main axis of the ellipse and the x-axis and the ellipticity γ (Fig. 1.6). Please note that the parameters Ψ' and Δ', which define here the polarization state of light, are in general not identical with the previously defined Ψ and Δ values, which describe how the sample changes the polarization. Only in the special historically important case, where the incident light is chosen 45° linearly polarized with respect to the plane of incidence, both parameter sets match. Commercially available ellipsometers determine Ψ and Δ independent from the selected incident polarization.

So far, all representations of the polarization are only applicable for totally polarized light. Hence, they represent 100 % linear, circular or elliptically polarized light and the constituting parameter pairs are of a well defined value. Unfortunately, this is sometimes not sufficient and it is necessary to consider also partial polarizations. Possible sources of partial polarized light are

- non ideal polarizers,
- lateral inhomogeneous samples (e.g. rough surfaces/interfaces or inhomogeneous film thickness),
- a divergent light beam (e.g. a short focal distance results in an uncertain angle of incidence),
- an insufficient spectral resolution and broad spectral line width, respectively.

Independent from the inbound polarization and the source of depolarization, partial polarization means that the well defined polarization is replaced by a statistical mixture of different polarization states. In this view the components of the Jones vector are now time dependent and polarization is measurable just as a time-average. A proper description of the partially polarized light requires therefore a third parameter which for example characterizes the probability w to find a certain polarization state. Related to the fact that effective intensities (time-averaged fields) are finally measured, the three constituting parameters are often expressed in terms of intensities. Complemented by the total intensity they form the 4 Stokes parameters [31]:

$$\begin{aligned} S_0 &= I, \\ S_1 &= I_x - I_y, \\ S_2 &= I_{+\pi/4} - I_{-\pi/4}, \\ S_3 &= I_l - I_r. \end{aligned} \tag{1.5}$$

The first Stokes parameter contains simply the total intensity I of the light. I_x, I_y, $I_{+\pi/4}$, and $I_{-\pi/4}$ are the intensities, which would pass through an ideal linear

polarizer oriented with the transmission axis in x, y, $+\pi/4$, and $-\pi/4$ direction, respectively. I_l and I_r are the intensities, which would pass through ideal left and right circular polarizers. The total intensity resumes to $I = I_x + I_y = I_{+\pi/4} + I_{-\pi/4} = I_l + I_r$. In case of totally polarized light $S_0^2 = S_1^2 + S_2^2 + S_3^2$, while for partially or unpolarized light $S_0^2 \geq S_1^2 + S_2^2 + S_3^2$. The degree of polarization is finally defined by:

$$P = \sqrt{\frac{S_1^2 + S_2^2 + S_3^2}{S_0^2}} = 2w - 1. \tag{1.6}$$

For more comprehensive descriptions of the different representations of polarized light and the relation among these representations we would refer at this point to respective literature about fundamental optics and ellipsometry [2, 4, 9, 32, 33]. Because of similarities in operational concepts to quantum physics, the theory of polarized light is furthermore discussed in a number of rather theoretical publications [11, 32, 34, 35]. An alternative description of partial polarized light by means of coherency-matrices is described for example in references [2, 36].

1.3.2.2 Jones and Mueller Matrix Methods

The matrix methods of Jones [30] and Mueller [37–40] are by far the most popular methods in order to describe the linear optical effects of polarizing optical elements. The Jones formalism is based on complex 2×2 matrices which are applied to the Jones vector as defined in the previous section. The Mueller matrix formalism uses 4×4 matrices with real elements which are applied to the Stokes parameters arranged now in a column vector $\bar{S} = (S_0, S_1, S_2, S_3)$. The impact of a polarizing element can thus be written as

$$\begin{pmatrix} E_x' \\ E_y' \end{pmatrix} = \hat{J} \begin{pmatrix} E_x \\ E_y \end{pmatrix} = \begin{pmatrix} J_{xx} & J_{xy} \\ J_{yx} & J_{yy} \end{pmatrix} \begin{pmatrix} E_x \\ E_y \end{pmatrix},$$
$$\begin{pmatrix} S_0' \\ S_1' \\ S_2' \\ S_3' \end{pmatrix} = \hat{M} \begin{pmatrix} S_0 \\ S_1 \\ S_2 \\ S_3 \end{pmatrix} = \begin{pmatrix} M_{00} & M_{01} & M_{02} & M_{03} \\ M_{10} & M_{11} & M_{12} & M_{13} \\ M_{20} & M_{21} & M_{22} & M_{23} \\ M_{30} & M_{31} & M_{32} & M_{33} \end{pmatrix} \begin{pmatrix} S_0 \\ S_1 \\ S_2 \\ S_3 \end{pmatrix}. \tag{1.7}$$

The complex 2×2 Jones matrix contains 8 parameters including the absolute phase which is not measurable. If the absolute phase and additionally the absolute intensity, which is also not if interest in ellipsometric measurements are ignored, the Jones matrix contains 6 relevant parameters that define the ability to change the polarization. All optical components and any arbitrarily anisotropic samples can be represented by means of these 6 parameters in a Jones matrix as long as no depolarization takes place.

The 16 coefficients of the Mueller matrix contain information about intensities passing through polarizing elements. This includes information about the absolute

intensity. Accordingly, the Mueller matrix contains 7 independent parameters, if no depolarization takes place. In turn this means that 9 identities exist among the 16 coefficients of a Mueller matrix in this case [39, 41]. It is thus feasible that the Mueller matrix of a non-depolarizing optical element can be calculated from the respective Jones matrix and vice versa except of the absolute phase [2, 42]. However, in case of depolarization the 16 coefficients of a Mueller matrix become independent and might include manifold orientation depending information about a sample. But notice, the polarization state of the obtained partially depolarized light is always fully characterized by only 3 parameters.

With the help of either the Jones or the Mueller matrix formalism it is now possible to calculate the measurable intensities for different orientations of the polarizing elements in an ellipsometer. Therefore, the matrix representations of all optical elements including the sample under investigation are multiplied in the respective order.

By a comparison of the measured intensities with those calculated, it is finally possible to obtain the unknown sample polarization transformation coefficients (PTC). The latter can be represented for example either by the bare Mueller or Jones matrix coefficients, the ellipsometric angles Ψ and Δ, or the (generalized) complex Fresnel coefficients. The choice of the most convenient representation depends on the sample under investigation and the specific ellipsometer type. Just like the choice which parameters are used, the determination of PTC's in practice also depends strongly on the sample properties and the ellipsometer type. If the intensity is for example continuously measured as a function of the rotation of a polarizing element it is often beneficial to consider the Fourier transformation of the measured sinusoidal signal. In case of an isotropic non-depolarizing sample, the two parameters describing the polarization probability are then encoded in the $\sin(2\alpha)$ and $\cos(2\alpha)$ Fourier coefficients and can be determined thereafter algebraically by a comparison of coefficients. According to the sampling theorem, it is also sufficient to measure the sinusoidal signal with a minimum of three fixed positions in order to obtain the two Fourier parameters in a fit algorithm. Finally, it is in some cases also possible to measure at four specific positions [4] and to calculate the two PTC's directly from the measured intensities.

1.3.3 Fresnel Coefficients

The second crucial step in an ellipsometric measurement now comprises the translation of the obtained PTC's to intrinsic sample properties like the dielectric function or the layer thickness (calculation step ② in Fig. 1.3). This problem of the light matter interaction could be rather complicated in case of increasingly complex sample structures. Therefore, only a few essential conclusions will be introduced which are typically used for analyzing organic film structures.

It is reasonable to consider organic and anorganic materials as homogeneous materials which are well characterized by its macroscopic optical properties i.e. the

macroscopic polarizability, dielectric function, or refractive index. This approximation is adequate as long as the wavelength is much larger than the size of the constituting molecules and larger than the unit cell of the crystal. It is often possible to assume a stratified sample structure, which allows a description of the light matter interaction with planar TEM waves. With these two assumptions it is possible to deduce complex reflection and transmission coefficients, which provide a link between the measured Ψ and Δ or PTC's and the intrinsic sample parameters. The sample parameters are usually determined within a fit procedure. This part of the data evaluation is often called "optical modeling". It is usually the most discriminating step in the data evaluation because it rests on a correctly assigned sample structure which has to be critical reviewed in advance.

1.3.3.1 Dielectric Function

The optical properties of a homogeneous material can be encountered in the macroscopic Maxwell equations i.e. the constitutive relations. These relations connect the macroscopic electric field $\boldsymbol{E}$ with the dielectric displacement $\boldsymbol{D}$ as well as the magnetic induction $\boldsymbol{B}$ and magnetic field $\boldsymbol{H}$ according to the polarization and magnetization of the material. Again, three simplifications can be used:

- In the optical frequency range the macroscopic magnetization is always zero.
- The discussed ellipsometric measurements comprise only linear optical effects and higher order contributions can be neglected.
- Spatial dispersion effects are negligible in homogeneous media.

As a result, the response of the material to an electric field is defined by the macroscopic polarizability P.[2] The material equations in a Fourier representation can be written as

$$\begin{aligned} \boldsymbol{D}[\omega] &= \varepsilon_0 \boldsymbol{E}[\omega] + \boldsymbol{P}\big[\boldsymbol{E}[\omega], \omega\big] \\ &= \varepsilon_0 \hat{\varepsilon}[\omega] \boldsymbol{E}[\omega], \\ \boldsymbol{B}[\omega] &= \mu_0 \boldsymbol{H}[\omega]. \end{aligned} \tag{1.8}$$

In optical problems the magnetic field strength is connected with the magnetic induction density just by the free space permeability μ_0. The macroscopic electric field strength is connected to the displacement density by the free space permittivity ε_0 and the dielectric tensor $\hat{\varepsilon}$ which depends on angular frequency ω. In absorbing materials $\hat{\varepsilon} = \hat{\varepsilon}_1 + i\hat{\varepsilon}_2$ is a complex tensor and the imaginary part of the tensor components is proportional to energy dissipation and thus to the absorption of the light. In case of isotropic media the dielectric tensor reduces to a scalar dielectric

[2] P is the spatial average of the induced dipole moments per unit volume.

Table 1.1 Equivalent quantities for the linear optical properties of homogeneous media

	Real part	Imaginary part
Dielectric function: ε	$\varepsilon_1 = n^2 - k^2$	$\varepsilon_2 = 2nk$
Refractive index: $\tilde{n} = \sqrt{\varepsilon}$	$n = \sqrt{(\varepsilon_1 + \sqrt{\varepsilon_1^2 + \varepsilon_2^2})/2}$	$k = \sqrt{(-\varepsilon_1 + \sqrt{\varepsilon_1^2 + \varepsilon_2^2})/2}$
Susceptibility: $\chi = \varepsilon - 1$	$\chi_1 = \varepsilon_1 - 1$	$\chi_2 = \varepsilon_2$
Optical conductivity: σ	$\sigma_1 = \omega\varepsilon_0\varepsilon_2$	$\sigma_2 = -\omega\varepsilon_0(\varepsilon_1 - 1)$
Loss function: $-\varepsilon^{-1}$	$\frac{-\varepsilon_1}{\varepsilon_1^2 + \varepsilon_2^2}$	$\frac{\varepsilon_2}{\varepsilon_1^2 + \varepsilon_2^2}$
Phase velocity: $v_p = c/\tilde{n}$	$\frac{1}{\sqrt{\varepsilon_0\mu_0}}\frac{1}{n}$	$\frac{1}{\sqrt{\varepsilon_0\mu_0}}\frac{1}{k}$

function.

$$\hat{\varepsilon} = \begin{pmatrix} \varepsilon & 0 & 0 \\ 0 & \varepsilon & 0 \\ 0 & 0 & \varepsilon \end{pmatrix} = \varepsilon \begin{pmatrix} 1 & 0 & 0 \\ 0 & 1 & 0 \\ 0 & 0 & 1 \end{pmatrix} \quad \text{(isotropic materials)}. \tag{1.9}$$

As already seen in (1.8) a couple of equivalent quantities can be used in order to describe the linear optical properties of a medium. Most widely used is the complex refractive index $\tilde{n} = n + ik$ where the real part n refers to the refractive index of transparent media. The imaginary part k is the absorption coefficient of a medium. Other common representations of the optical response function and the relations among them are summarized in Table 1.1.

In case of an anisotropic sample with three intrinsic Cartesian optical axes the dielectric tensor can be diagonalized in the form

$$\hat{\varepsilon} = \begin{pmatrix} \varepsilon_x & 0 & 0 \\ 0 & \varepsilon_y & 0 \\ 0 & 0 & \varepsilon_z \end{pmatrix} \quad \text{(anisotropic materials)}. \tag{1.10}$$

The dielectric tensor is defined now by three independent dielectric functions ε_x, ε_y, and ε_z which determine the different polarizabilities for electric fields in the corresponding directions. Such a matrix is suitable for biaxial crystals of e.g. triclinic, monoclinic, and orthorhombic symmetry. Uniaxial crystals of e.g. hexagonal, tetragonal, trigonal, and rhombohedral symmetry are defined analogue but only with two independent components [43]. As indicated before, in isotropic materials e.g. cubic crystals, all components are equal. If the sample is placed in an arbitrary orientation in the ellipsometer, the matrix (1.10) has to be transposed by a rotation about the Euler angles.

Organic molecules like sugar, however, have often an intrinsic handedness/chirality. This yields an optical activity and circular dichroism if light is transmitted through a film or liquid solution. The dielectric tensor of such materials is now no longer symmetric. But in case of vanishing absorption (optical activity) the tensor

is still Hermitian ($\varepsilon_{ij} = \varepsilon_{ij}*$). The constitutive Maxwell relation is than written as

$$\boldsymbol{D}[\omega] = \varepsilon_a \boldsymbol{E}[\omega] + i\varepsilon_0 \boldsymbol{G}[\omega] \times \boldsymbol{E}[\omega], \tag{1.11}$$

where ε_a is the dielectric tensor for vanishing optical activity. The vector $\boldsymbol{G}$ is pointing in the direction of the light propagation and is called the gyration vector [44].

The optical rotation due to the Faraday effect which may emerge in the presents of a magnetic field is defined analogously [43, 44]

$$\boldsymbol{D}[\omega] = \varepsilon_a \boldsymbol{E}[\omega] + i\varepsilon_0 \gamma \boldsymbol{B}[\omega] \times \boldsymbol{E}[\omega]. \tag{1.12}$$

1.3.3.2 Fresnel Equations

As mentioned before the link between sample properties like the dielectric function and its polarization properties given either by Ψ and Δ or by the PTC's can be obtained by the definition of reflection and transmission coefficients. These complex coefficients determine to which amount the electric field amplitudes of the incident s- and p-polarization component are attributed to the respective fields in the reflected and transmitted beam and determine the relative phase shifts among these components.

For a single interface between two isotropic homogeneous media these relations can be obtained as a result of the boundary conditions committed by the Maxwell equations. They are known as the Fresnel equations of the form

$$\begin{aligned} r_p &= \frac{\tilde{n}_2 \cos\varphi_i - \tilde{n}_1 \cos\varphi_t}{\tilde{n}_2 \cos\varphi_i + \tilde{n}_1 \cos\varphi_t}, \\ r_s &= \frac{\tilde{n}_1 \cos\varphi_i - \tilde{n}_2 \cos\varphi_t}{\tilde{n}_1 \cos\varphi_i + \tilde{n}_2 \cos\varphi_t}, \\ t_p &= \frac{2\tilde{n}_1 \cos\varphi_i}{\tilde{n}_2 \cos\varphi_i + \tilde{n}_1 \cos\varphi_t}, \\ t_s &= \frac{2\tilde{n}_1 \cos\varphi_i}{\tilde{n}_1 \cos\varphi_i + \tilde{n}_2 \cos\varphi_t}. \end{aligned} \tag{1.13}$$

$\tilde{n}_1$ and $\tilde{n}_2$ are the complex refractive indices of the incident and refractive media, respectively, and the angles of incidence φ_i and refraction φ_t are described by Snell's law ($\tilde{n}_1 \sin\varphi_i = \tilde{n}_2 \sin\varphi_t$).

The assumption of a sample, which consists of only a single perfectly smooth surface, is unfortunately very unrealistic. In practice at least unintentional surface overlayers or a finite surface roughness are not negligible. Nevertheless, the Fresnel equations are often used as a good approximation. The obtained dielectric function is then the so-called pseudo dielectric function [6].

$$\langle\varepsilon\rangle = \sin^2\phi\left(1 + \tan^2\phi\left(\frac{1-\rho}{1+\rho}\right)^2\right), \quad \rho = \frac{r_p}{r_s} = \tan\Psi e^{i\Delta}. \tag{1.14}$$

1.3.3.3 Homogeneous Stratified Media

A simple optical layer model of practical importance describes a single isotropic layer (l) of the complex refractive index $\tilde{n}_l$ and thickness d on a substrate (s) with the complex refractive index $\tilde{n}_s$. Light, which incidences from the ambient (a) with the refractive index n_a, is reflected on the surface and the interface between layer and substrate. Due to multiple reflections within the layer, the overall reflected electric fields parallel and perpendicular to the plane of incidence add up by a geometric series. The summations gives the Airy formula for the so-called 3-phase model [2, 17, 44–46]:

$$\begin{aligned} r_p &= \frac{r_{al_p} + r_{ls_p} e^{i2\beta}}{1 + r_{al_p} r_{ls_p} e^{i2\beta}}, \\ r_s &= \frac{r_{al_s} + r_{ls_s} e^{i2\beta}}{1 + r_{al_s} r_{ls_s} e^{i2\beta}}, \end{aligned} \tag{1.15}$$

where $r_{al_{p/s}}$ and $r_{ls_{p/s}}$ are the Fresnel reflection coefficients on the ambient layer boundary and the layer substrate boundary, respectively (1.13). The phase factor β is given by

$$\beta = \frac{2\pi}{\lambda} d \sqrt{n_l^2 - n_a^2 \sin^2 \phi_a} = \frac{2\pi}{\lambda} (d\, n_l) \cos \phi_l. \tag{1.16}$$

λ is the wavelength of the light in vacuum and ϕ_a the angle of incidence. It will be shown later that generalized complex "Fresnel" coefficients as defined in Eq. (1.15) can be obtained also for complex anisotropic structures. Before it should be mentioned that the reflection coefficients of the 3-phase model contain already 5 parameters which determine the optical properties of the sample. Even if the substrate dielectric function is known, we have already one parameter more than a single measurement at a given angle of incidence can deliver. An examination of the phase factor β furthermore illustrates the coupling of n_l and d. An unambiguous determination of the thickness and the optical properties is possible by means of multiple angle of incidence measurements. A solution for very thin layers with $d \ll 1$ nm will be discussed in Chap. 10.

The problem of a multilayer structure with planar parallel interfaces can be solved with the help of a 2×2 transfer matrix methods [2, 44, 47–51]. To some extend similar to the Jones matrix formalism, it is possible to connect the electric fields of the forward and backward traveling waves at each interface by a transfer matrix which is defined by the Fresnel coefficients for this specific interface and thus depends on the refractive index on both sides as well as the incident angle. In contrast to the Jones matrix formalism the distance between the interfaces is assumed now to be smaller than the coherence length of the light and interference between the forward and backward traveling waves becomes possible. Consequently, a propagation matrix has to be introduced, which implements a (complex) phase factor to the electric fields crossing a given layer. The reflection and transmission coefficients (r_p/r_s and t_p/t_s) of the whole slab are finally obtained by the product of all transfer and propagation matrices in the respective order.

Table 1.2 Reflection coefficients for parallel and perpendicular polarized light reflected at the surface of an uniaxial anisotropic material if the optical axis c coincides with one of the three high symmetry orientations [2, 52]. ($c \parallel x$)—c parallel to the plane of incidence and the surface; ($c \parallel y$)—c perpendicular to the plane of incidence and parallel to the surface; ($c \parallel z$)—c perpendicular to the surface and parallel to the plane of incidence. $\varepsilon_\perp$ and $\varepsilon_\parallel$ correspond to the dielectric tensor components perpendicular and parallel to the optical axis i.e. the ordinary and extraordinary dielectric function

	p polarization (r_{pp})	s polarization (r_{ss})
($c \parallel x$):	$\dfrac{\sqrt{\varepsilon_\perp \varepsilon_\parallel}\cos\phi_i - \sqrt{\varepsilon_\perp - \sin^2\phi_i}}{\sqrt{\varepsilon_\perp \varepsilon_\parallel}\cos\phi_i + \sqrt{\varepsilon_\perp - \sin^2\phi_i}}$	$\dfrac{\cos\phi_i + \sqrt{\varepsilon_\perp - \sin^2\phi_i}}{\cos\phi_i - \sqrt{\varepsilon_\perp - \sin^2\phi_i}}$
($c \parallel y$):	$\dfrac{\varepsilon_\perp\cos\phi_i - \sqrt{\varepsilon_\perp - \sin^2\phi_i}}{\varepsilon_\perp\cos\phi_i + \sqrt{\varepsilon_\perp - \sin^2\phi_i}}$	$\dfrac{\cos\phi_i + \sqrt{\varepsilon_\parallel - \sin^2\phi_i}}{\cos\phi_i - \sqrt{\varepsilon_\parallel - \sin^2\phi_i}}$
($c \parallel z$):	$\dfrac{\sqrt{\varepsilon_\parallel \varepsilon_\perp}\cos\phi_i - \sqrt{\varepsilon_\parallel - \sin^2\phi_i}}{\sqrt{\varepsilon_\parallel \varepsilon_\perp}\cos\phi_i + \sqrt{\varepsilon_\parallel - \sin^2\phi_i}}$	$\dfrac{\cos\phi_i + \sqrt{\varepsilon_\perp - \sin^2\phi_i}}{\cos\phi_i - \sqrt{\varepsilon_\perp - \sin^2\phi_i}}$

1.3.3.4 Anisotropic Media

It is a common property of isotropic media that the reflected and transmitted electric field components parallel and perpendicular to the plane of incidence are independent. Accordingly, the previously defined Fresnel equations and the Airy formulas handle both components independently. Incident light with parallel polarization is not converted by reflection or transmission to perpendicular polarized light and vice versa perpendicular polarized light does not contribute to the parallel polarization. This separation retains also for anisotropic materials as long as the principal optical axes as defined in Eq. (1.10) are aligned parallel or perpendicular to the plane of incidence and the sample surface. For such high symmetry configurations it is possible to deduce reflection coefficients analogous to the classical Fresnel equations or the Airy formulas [2, 52]. Solutions for an uniaxial anisotropic bulk sample are summarized in Table 1.2. Solutions for anisotropic layer structures can be found in reference [2, 52]. The dependency on the sample orientations shows that the measurement of only one Ψ and Δ pair is not sufficient anymore. Unambiguous results are obtained by measuring in different sample orientations and with different angles of incidence. Thus, sensitivity to an out of plane anisotropy is obtained with a variation of the incidence angle while an in-plane anisotropy requires measurements with different azimuthal sample orientations (q.v. Chaps. 7 and 10).

Aspnes [53] has described a solution for the pseudo dielectric function $\langle\varepsilon\rangle$ (Eq. (1.14)) measured on a biaxial crystal. Based on a first-order expansion, which assumes that the anisotropies are small corrections to an isotropic mean value, he

obtained

$$\langle\varepsilon\rangle = \varepsilon + \frac{\varepsilon - \sin^2\phi_0}{(\varepsilon-1)\sin^2\phi_0}\Delta\varepsilon_x - \frac{\varepsilon\cos^2\phi_0 - \sin^2\phi_0}{(\varepsilon-1)\sin^2\phi_0}\Delta\varepsilon_y - \frac{1}{\varepsilon-1}\Delta\varepsilon_z, \quad \text{where}$$
$$\varepsilon_x = \varepsilon + \Delta\varepsilon_x, \quad \varepsilon_y = \varepsilon + \Delta\varepsilon_y, \quad \text{and} \quad \varepsilon_z = \varepsilon + \Delta\varepsilon_z. \tag{1.17}$$

This relation is not exact, but reveals the very small influence of the ε_z component normal to the surface, if $|\varepsilon|$ is moderately large. The physical reason is simple. If the material is optically thick ($n_0 \ll n_1$), the incoming light is refracted in the direction of the surface normal and the electric and magnetic field vectors in the material are mostly parallel to the surface. Therefore, it is difficult to measure $\varepsilon_\parallel$ if the optical axis (c-axis) is perpendicular to the sample surface and the sample. On the other hand it shows that the anisotropy can often be neglected and the use of an isotropic model yields reasonable results.

In arbitrary anisotropic materials or for arbitrary sample orientation p- and s-polarizations couple to each other. As a consequence, the previously discussed Fresnel equations as well as the shortly introduced 2×2 transfer matrix methods are in this case not applicable anymore. Additionally to the mode coupling between the reflected electric field components, the field evolution inside an anisotropic layer depends now on the propagation direction. A solution for this problem was introduced by Teiler, Henvis, and Berreman [54–58] by a 4×4 transfer matrix formalism. As a result on can obtain generalized reflection coefficients (r_{pp}, r_{ss}, r_{ps}, and r_{sp}) [52, 57] which may are used as the polarization transformation coefficients (PTC).

1.4 Dielectric Properties

1.4.1 Dispersion Models—Lorentz Oscillator

It is by far impossible to provide a common description of the dielectric properties neither for inorganic [33, 59] nor for organic materials [60]. Nevertheless, a relatively good insight could be obtained with some classical considerations. It was mentioned already that the optical properties i.e. the dielectric function rises from the polarizability of the material. Polarizable entities in an organic layer may are the individual molecules were a dipole moment is induced by the electric field of the incident light. In the infrared spectral region this could be obtained by a vibration of ions in the molecule i.e. phonons. In the visible and UV it is mainly the excitation of electrons (excitons) which gives a dipole moment. Both excitations can be described classically by a mechanical harmonic oscillators of a negative and positive charge with the equation of motion. Because of the strong localization of electrons in the individual molecules, organic layers can be treated as a ensemble of uncoupled oscillators. Within the Lorentz oscillator model the time dependent dipole moment of all entities is translated in a polarization density and one can obtain an expression

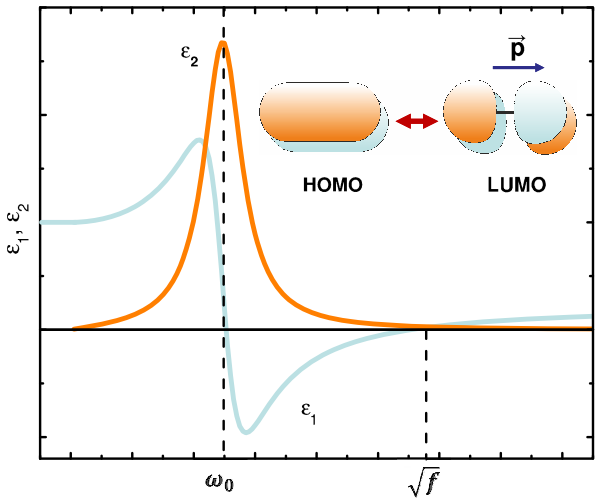

Fig. 1.7 Real and imaginary part of the dielectric function calculated within the classical Lorentz oscillator model for a single resonance. Such a resonance could be the electronic excitation from the highest occupied molecular orbital (HOMO) to the lowest unoccupied molecular orbital (LUMO) which induces a dipole moment p

for the dielectric function of a single oscillator (Fig. 1.7)

$$\varepsilon[\omega] = 1 + \frac{f}{\omega_0'^2 - \omega^2 - i\omega\gamma} = 1 + \frac{N}{\varepsilon_0}\alpha[\omega]. \tag{1.18}$$

ω_0' is the resonance frequency of the oscillator and γ the damping factor related to energy dissipation e.g. by scattering precesses. The oscillator strength f is proportional to the number of oscillators per unit volume N while α is the polarizability of each entity. The excitation of free electrons in metallic materials is given in this model by an oscillator with a resonance frequency $\omega_0 = 0$.

The assumption of totally uncoupled oscillators is of course a very crude approximation. In dense organic layers each molecular dipole is screened at least by the surrounding molecules. Taking this effect into account the dielectric function of isotropic materials is rather given by the Clausius-Mosotti or Lorentz-Lorenz equation [33, 59]

$$\frac{\varepsilon - 1}{\varepsilon + 2} = \frac{N\alpha}{3\varepsilon_0}. \tag{1.19}$$

For a small damping one can find the same expression as in Eq. (1.18) but with a slightly shifted eigenfrequency

$$\varepsilon[\omega] = 1 + \frac{f}{\omega_0^2 - \omega^2 - i\omega\gamma} \quad \text{where } \omega_0^2 = \omega_0'^2 - \frac{f}{3}. \tag{1.20}$$

This effect is observed as a red shift of absorption structures while going from gas phase or diluted materials to thin films and finally to bulk materials. In anisotropic molecular crystals on can observe the so-called Davydov splitting due to different screening components (q.v. Chap. 9 (O. Gordan et al.)).

Organic molecules of course possess not only one oscillator but a couple of different phonon and exciton dipole excitations. Therefore, the whole dielectric function has finally to be approximated by a sum of oscillators:

$$\varepsilon[\omega] = 1 + \sum_n \frac{f_n}{\omega_{0n}^2 - \omega^2 - i\omega\gamma_n}. \tag{1.21}$$

Most of the organic molecules are additionally highly anisotropic. The dipole moments of the different phonon and exciton excitations are usually linked to a certain direction in the molecule and thereby only measurable for respective electric field components. It is of particular importance that different oscillators may emerge in arbitrary orientations (q.v. Chap. 3). This anisotropy does not necessarily lead to an optical anisotropy of the material if the molecules are randomly arranged. However, in ordered arrangements, i.e. organic crystals or due to an interface specific bonding, the molecular anisotropy could appear in different aspects. Hereby, the anisotropy of the single molecules is largely conserved. The reason is the strong localization of the electrons within the molecule in contrast to metals and semiconductors. As a consequence it is not always possible to diagonalize the dielectric tensor (Eq. (1.10)) for all wavelengths simultaneously.

Beside the introduced Lorentz oscillator model one can find a huge number of other dispersion relations in literature derived from classical electrodynamic, quantum mechanical, or just empirical consideration. Because of its relevance in the thin film analysis only the model of Cauchy should be briefly mentioned here in addition [61]. The latter describes the refractive index n of a material in the transparent region as a Taylor series in ω^2. The benefit of this model is that it can be used to determine a layer thickness from a spectroscopic ellipsometric measurement. The knowledge about the dispersion of n derived from the Kramers-Kronig relations solves here the problem of parameter coupling between n and the thickness d.

1.4.2 Inhomogeneous Media and Structured Interfaces

Effective medium approximations (EMA) are used in order to obtain effective dielectric properties for inhomogeneous layers composed of different materials in a certain geometrical arrangement. Such a substitution of heterogeneous media by effective material is possible if

- the constituent particles are smaller than the wavelength (beside the host material),
- but big enough so that dielectric properties of the constituting materials are still the same,

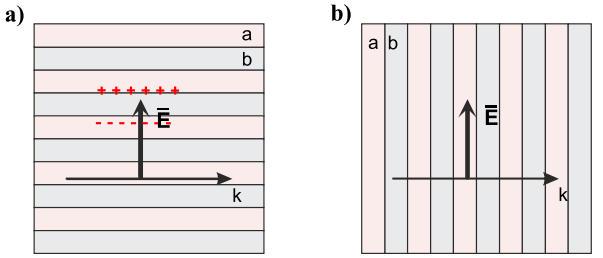

Fig. 1.8 The effective dielectric function of two media a and b can be calculated within effective medium approximations depending on the topology of mixing. All the different solutions, however, are found between the so-called Wiener bounds (**a**) for a stratified structure parallel to the electric field with maximal screening ($\frac{1}{\langle\varepsilon\rangle} = \frac{f_a}{\varepsilon_a} + \frac{f_b}{\varepsilon_b}$) and (**b**) for a stratified structure perpendicular to the electric field without screening ($\langle\varepsilon\rangle = f_a\varepsilon_a + f_b\varepsilon_b$)

- and if constituent particles are randomly distributed (diffraction and spatial dispersion effects are negligible).

The theory considers local field effects due to the surrounding media and the attendant screening. The effective dielectric function is thus NOT an average of the different constituting material dielectric functions. It can be shown that the effective medium properties are rather than a sum of the respective polarizabilities α_n. The effective dielectric function is given by an expression similar to the Clausius-Mosotti relation (1.19) [62]

$$\frac{\varepsilon - \varepsilon_h}{\varepsilon + p\varepsilon_h} = \sum_n f_n \frac{\varepsilon_n - \varepsilon_h}{\varepsilon_n + p_n\varepsilon_h} \tag{1.22}$$

where p is the so-called depolarization factor with

$$\begin{aligned} p &= 0 \quad \text{no screening,} \\ p &= 1 \quad \text{2D cylindrical inclusions,} \\ p &= 2 \quad \text{3D spherical inclusions,} \\ p &\to 1 \quad \text{maximal screening.} \end{aligned}$$

f_n is the volume fraction of the different components. In (1.22) the host material is defined with the dielectric function ε_h while the Clausius-Mosotti relation (1.19) is using $\varepsilon_h = 1$. The effect of the different depolarization factors is probably best seen by inspecting the extreme cases of none and maximum screening in layered structures, the so-called Wiener bounds (Fig. 1.8).

Table 1.3 summarizes three common EMA solutions for certain configurations. Especially the Bruggeman solution is widely used. Here, we would mention in particular the possibility to mimic a rough surface or interface by means of an effective medium layer [63]. The layer thickness could be determined, if necessary, by atomic force microscopy (AFM). In the visible spectral range the thickness of the effective medium layer corresponds approximately to the root-mean-square (rms) roughness

Table 1.3 Most common effective medium approximations

Bruggeman [65]	$0 = f\frac{\varepsilon_a - \langle\varepsilon\rangle}{\varepsilon_a + 2\langle\varepsilon\rangle} + (1-f)\frac{\varepsilon_b - \langle\varepsilon\rangle}{\varepsilon_b + 2\langle\varepsilon\rangle}$	randomly mixed particles
Maxwell-Garnett [66]	$\frac{\langle\varepsilon\rangle - \varepsilon_M}{\langle\varepsilon\rangle + 2\varepsilon_M} = f\frac{\varepsilon_p - \varepsilon_M}{\varepsilon_p + 2\varepsilon_M}$	isolated particles in a matrix
Looyenga [67]	$\sqrt[3]{\langle\varepsilon\rangle} = f\sqrt[3]{\varepsilon_a} + (1-f)\sqrt[3]{\varepsilon_b}$	heterogeneous mixtures

determined in scan range of about 5 × 5 µm [64]. Further applications are described in Chap. 6 (T.W.H. Oates).

1.5 Ellipsometric Configurations

With increasing amount of different analytical issues and the progress in the technical possibilities, by time also various types of ellipsometric systems have been developed. They differ mainly in the way how the polarization state of the incident light is generated and how the resulting polarization is analyzed (Fig. 1.1). Depending on the analytical requirements, the sensitivity and measurement speed can be optimized by choosing one or the other configuration [68]. Other modifications are made in order to increase the interface sensitivity for instance by attenuated/internal total reflectance (ATR/TIR) and internal total reflection (Chap. 12, H. Arwin).

1.5.1 Null-Ellipsometer

A "Null-Ellipsometer" is one of the oldest configurations. It consists of three polarizing elements. Two linear polarizing elements, namely the polarizer (*P*) and the analyzer (*A*) as well as a compensator (*C*). The compensator is placed either between the polarizer and the sample (*PCSA*-configuration) or between the sample and the analyzer (*PSCA*-configuration). As indicated already by the name, sample properties are determined by varying (rotating) two of the three components until the measured intensity is minimized. With this procedure the ellipsometric angles Ψ and Δ can be directly obtained [69]. The involved nulling procedure is on the other hand a huge disadvantage although the rotation of the polarizers can be meanwhile motorized. Furthermore, all wavelength have to be measured one after another and a parallelization is hardly possible.

1.5.2 Rotating Polarizer/Analyzer

The rotating polarizer/analyzer ellipsometer is a photometric configuration, which was used in the first automatic spectroscopic systems [19]. In this *PSA* configuration either the polarizer (*PSA-RPE*) or the analyzer (*PSA-RAE*) is rotated. Both

the continuous and the so-called "step scan" rotations are used. It was mentioned already in Sect. 1.3.2.2 that Ψ and Δ are obtained by analyzing the sinusoidal detector signal in terms of the $\sin(2\alpha)$ and $\cos(2\alpha)$ Fourier coefficients. The decision whether the polarizer or the analyzer is rotated depends on the used light source and the position of the monochromator. Hereby, polarization effects of the peripheric components are minimized. The "step scan" mode is usually used in connection with spectrographs and interferometric setups where all wavelengths are recorded in parallel.

With this type of ellipsometer it is possible to determine dielectric functions and layer thicknesses of isotropic or anisotropic absorbing materials with high accuracy. Incident angle scans (variable angle spectroscopic ellipsometry) provide enhanced sensitivity to layer thicknesses or out-of-plane anisotropies. Azimuthal rotation of the sample allows the determination of in-plane anisotropies. A general advantage is the reduced number of optical elements which minimizes alignment errors. Disadvantages arise from sensitivity limitations in case of transparent or metallic samples. Furthermore it is not possible to determine the sign of Δ or to distinguish between circular and unpolarized light. Thus depolarization effects can not directly measured.

1.5.3 Rotating Compensator

In a rotating compensator ellipsometer the linear polarizing elements are fixed and a rotating compensator is added either in *PCSA* or in the *PSCA* arrangement. With these modification, errors due to polarization dependent detectors or polarized light sources are avoided. The ellipsometric angles Ψ and Δ are now decoded in the 2α and 4α Fourier coefficients of the recorded detector signal [68, 70]. In addition it is possible to determine depolarizations i.e. all four Stokes parameters (Eq. (1.5)). Moreover, it is now possible to determine Δ with the correct sign and with higher precision in comparison to rotating analyzer systems. Problems mainly arise in connection with the necessary calibration of the compensator. Quarter wave plates are applicable only for one wavelength and even "achromatic" compensator plates feature a distinct wavelength dependence.

Additional information are obtained if also the polarizer is rotated. In these generalized ellipsometric measurements all 6 polarization transformation coefficients (PTC) of a non-depolarizing arbitrary anisotropic sample i.e. the 6 independent Jones matrix coefficients (Eq. (1.7)) can be determined. In case of depolarization one can gain maximal 12 parameters i.e. the first three rows of the Mueller matrix (Eq. (1.7)).

1.5.4 Photo-Elastic Modulator Ellipsometer

In these kinds of ellipsometers, a photo-elastic modulator (PEM) is used instead of compensator. The modulation yields here a time dependent change of the retarda-

tion. This is achieved technically by a resonant acoustic excitation of an isotropic crystal [71, 72]. The generated modulation is thus typically in the 100 kHz range. By using a PEM instead of the rotating compensator the scan speed is therefore much higher. Also the problem of wobbling light beams is avoided because the system do not contain moving parts. Drawbacks are again the wavelength dependency of the retardation and a fragile calibration of the PEM.

1.5.5 Dual Rotating Compensator

The dual rotating compensator configuration (*PCSCA*) extents the possibilities of the generalized ellipsometry even further. This method is also known as "Mueller matrix" ellipsometry. Quite in general it technically supports the determination of all Mueller matrix coefficients (Eq. (1.7)) [42, 73, 74]. In practice, however, many of them are not independent from each other and the interpretation of the measured Mueller matrix elements in terms of intrinsic physically meaningful sample parameters is a demanding problem. Mueller matrix measurements recorded at different incidence angles and different azimuthal sample orientations may provide perhaps most comprehensive information about the optical response even for complex sample structures [75, 76].

1.5.6 Reflection Anisotropy Spectroscopy

Reflection anisotropy spectroscopy (RAS) is a polarimetric method closely related to ellipsometry with a specific surface and interface sensitivity. It differs only by the angle of incidence which is chosen perpendicular to the sample surface ($\varphi = 90°$). A standard configuration compares, apart from that, to the photo-elastic modulator ellipsometer [77, 78]. In this configuration the polarization of the incidence light does not change upon reflection as long as the sample is isotropic (amorphous glass or cubic crystals like those of Si and Cu). The collected signal at the detector is constant. Any anisotropic surface or self organized anisotropic add-layer of molecules creates a modulation, which can be recorded with very high sensitivity for example with a lock-in amplifier [79–81].

References

1. H.G. Tompkins, E.A. Irene, *Handbook of Ellipsometry* (William Andrew, Norwich, 2005)
2. R.M.A. Azzam, N.B. Bashara, *Ellipsometry and Polarized Light*. (North-Holland, Amsterdam, 1987). Paperback edn.
3. H.G. Tompkins, *A User's Guide to Ellipsometry* (Academic Press, San Diego, 1993)
4. A. Röseler, *Infrared Spectroscopic Ellipsometry* (Akademie-Verlag, Berlin, 1990)

5. U. Rossow, W. Richter, in *Optical Characterization of Epitaxial Semiconductor Layers*, ed. by G. Bauer, W. Richter (Springer, Berlin, 1996), pp. 68–128
6. D.E. Aspnes, in *Handbook of Optical Constants of Solids*, vol. I, ed. by E.D. Palik (Academic Press, Amsterdam, 1985), pp. 89–112
7. D.E. Aspnes, in *Optical Properties of Solids: New Developments*, ed. by B. Seraphin (North-Holland, Amsterdam, 1975)
8. R.M.A. Azzam, Surf. Sci. **56**, 6 (1976)
9. J. Tinbergen, *Astronomical Polarimetry* (Cambridge University Press, Cambridge, 1996)
10. T. Novikova, A. De Martino, S.B. Hatit, B. Drévillon, Appl. Opt. **45**, 3688 (2006)
11. M.C. Britton, Astrophys. J. **532**, 1240 (2008)
12. J.C. Jamin, Ann. Chim. Phys. **19**, 296 (1847)
13. W. Wernicke, Ann. Phys. (Leipz.) **266**, 452 (1887)
14. W. Voigt, Ann. Phys. (Leipz.) **267**, 326 (1887)
15. A. Rothen, Rev. Sci. Instrum. **16**, 26 (1945)
16. P. Drude, Ann. Phys. (Leipz.) **272**, 865 (1889)
17. P. Drude, Ann. Phys. (Leipz.) **272**, 532 (1889)
18. P. Drude, Ann. Phys. **39**, 481 (1890)
19. D.E. Aspnes, A.A. Studna, Appl. Opt. **14**, 220 (1975)
20. J.E. Greene, A.C. Boccara, C. Pickering, J. Rivory (eds.), *Proceedings of the 1st International Conference on Spectroscopic Ellipsometry*. Thin Solid Films, vol. 234 (Elsevier, Amsterdam, 1993)
21. R.W. Collins, D.E. Aspnes, E.A. Irene (eds.), *Proceedings of the 2nd International Conference on Spectroscopic Ellipsometry*. Thin Solid Films, vol. 313–314 (Elsevier, Amsterdam, 1998)
22. M. Fried, K. Hingerl, J. Humlíček (eds.), *Proceedings of the 3rd International Conference on Spectroscopic Ellipsometry*. Thin Solid Films, vol. 455–456 (Elsevier, Amsterdam, 2004)
23. H. Arwin, U. Beck, M. Schubert (eds.), *Proceedings of the 4th International Conference on Spectroscopic Ellipsometry* (Wiley/VCH, Weinheim, 2008)
24. H.G. Tompkins (ed.), *Proceedings of the 5th International Conference on Spectroscopic Ellipsometry*. Thin Solid Films, vol. 11 (Elsevier, Amsterdam, 2011)
25. A. Rothen, in *Ellipsometry in the Measurement of Surfaces and Thin Films*, ed. by R.R. Stromberg, J. Kruger, E. Passaglia (Natl. Bur. of Standards, Washington, 1963), pp. 7–24
26. K. Vedam, Thin Solid Films **313–314**, 1 (1998)
27. M. Schubert, Ann. Phys. **15**, 480 (2006)
28. R.M.A. Azzam, Thin Solid Films **519**, 2584 (2011)
29. E.A. Irene, in *Ellipsometry at the Nanoscale*, ed. by M. Losurdo, K. Hingerl (Springer, Heidelberg, 2013), pp. 1–30
30. R.C. Jones, J. Opt. Soc. Am. **31**, 493 (1941)
31. G.G. Stokes, Trans. Camb. Philos. Soc. **9**, 399 (1852)
32. J. Humlíček, in *Handbook of Ellipsometry*, ed. by H.G. Tompkins, E.A. Irene (William Andrew, Norwich, 2005), pp. 3–90
33. M. Born, E. Wolf, *Principles of Optics*, 5th edn. (Pergamon Press, Oxford, 1975)
34. C. Brosseau, *Fundamentals of Polarized Light—A Statistical Optics Approach* (Wiley, New York, 1998)
35. U. Fano, J. Opt. Soc. Am. **39**, 859 (1949)
36. R. Barakat, J. Opt. Soc. Am. **53**, 317 (1963)
37. H. Mueller, J. Opt. Soc. Am. **38**, 661 (1948)
38. P. Soleillet, Ann. Phys. **12**, 23 (1929)
39. R.C. Jones, J. Opt. Soc. Am. **37**, 107 (1947)
40. M.J. Walker, Am. J. Phys. **22**, 170 (1954)
41. G.E. Jellison, in *Handbook of Ellipsometry*, ed. by H.G. Tompkins, E.A. Irene (William Andrew, Norwich, 2005), pp. 237–296
42. F. Le Roy-Brehonnet, B. Le Jeune, Prog. Quantum Electron. **21**, 109 (1997)
43. M. Schubert, in *Handbook of Ellipsometry*, ed. by H.G. Tompkins, E.A. Irene (William Andrew, Norwich, 2005), pp. 637–717

44. P. Yeh, *Optical Waves in Layered Media* (Wiley, New York, 1988)
45. G.B. Airy, Philos. Mag. Ser. 7 **3**(2), 20 (1833)
46. H. Hauschild, Ann. Phys. **63**, 816 (1920)
47. F. Abeles, Ann. Phys. Paris **5**, 596 (1950)
48. P.H. Berning, in *Physics of Thin Films*, vol. I, ed. by G. Hass (Academic Press, New York, 1963)
49. J. Humlíček, Opt. Acta **30**, 97 (1983)
50. C.J. Laan, H.J. Frankena, Appl. Opt. **17**, 538 (1978)
51. M.V. Klein, T.E. Furtak, *Optics* (Wiley, New York, 1986)
52. M. Schubert, Phys. Rev. B **53**, 4265 (1996)
53. D.E. Aspnes, J. Opt. Soc. Am. **70**, 1275 (1980)
54. S. Teitler, B.W. Henvis, J. Opt. Soc. Am. **60**, 830 (1970)
55. D.W. Berreman, T.J. Scheffer, Phys. Rev. Lett. **25**, 577 (1970)
56. D.W. Berreman, J. Opt. Soc. Am. **62**, 502 (1972)
57. P. Yeh, Surf. Sci. **96**, 41 (1980)
58. H. Wöhler, G. Haas, M. Fritsch, D.A. Mlynski, J. Opt. Soc. Am. A **5**, 1554 (1988)
59. C.F. Klingshirn, *Semiconductor Optics* (Springer, Berlin, 1997)
60. M. Pope, C.E. Swenberg, *Electronic Processes in Organic Crystals and Polymers* (Oxford University Press, New York, 1999)
61. M.A.L. Cauchy, *Memoire sur la dispersion de la lumiere* (Calve, Prague, 1863)
62. D.E. Aspnes, Am. J. Phys. **50**, 704 (1982)
63. D.E. Aspnes, J.B. Theeten, Phys. Rev. B (1979)
64. J. Koh, Y. Lu, C.R. Wronski, Y. Kuang, R.W. Collins, Physics **69**, 1297 (1996)
65. D.A.G. Bruggeman, Ann. Phys. **5**, 636 (1935)
66. J.C. Maxwell-Garnett, Philos. Trans. R. Soc. Lond. Ser. A, Math. Phys. Sci. **203**, 385 (1904)
67. H. Looyenga, Physica **31**, 401 (1965)
68. D.E. Aspnes, Thin Solid Films **455–456**, 3 (2004)
69. F.L. McCrackin, E. Passaglia, R.R. Stromberg, H.L. Steinberg, J. Res. Natl. Bur. Stand. A, Phys. Chem. **67A**, 363 (1963)
70. M. Dressel, B. Gompf, D. Faltermeier, A.K. Tripathi, J. Pflaum, M. Schubert, Opt. Express **16**, 19770 (2008)
71. S.N. Jasperson, Rev. Sci. Instrum. **40**, 761 (1969)
72. O. Acher, E. Bigan, B. Drevilion, Rev. Sci. Instrum. **60**, 65 (1989)
73. R.W. Collins, J. Koh, J. Opt. Soc. Am. A **16**, 1997 (1999)
74. M.H. Smith, Appl. Opt. **41**, 2488 (2002)
75. M. Losurdo, M. Bergmair, G. Bruno, D. Cattelan, C. Cobet, A. de Martino, K. Fleischer, Z. Dohcevic-Mitrovic, N. Esser, M. Galliet, R. Gajic, D. Hemzal, K. Hingerl, J. Humlíček, R. Ossikovski, Z.V. Popovic, O. Saxl, J. Nanopart. Res. **11**, 1521 (2009)
76. B. Gompf, J. Braun, T. Weiss, H. Giessen, M. Dressel, U. Hübner, Phys. Rev. Lett. **106**, 185501 (2011)
77. D.E. Aspnes, A.A. Studna, Phys. Rev. Lett. **54**, 1956 (1985)
78. D.E. Aspnes, J.P. Harbison, A.A. Studna, L.T. Florez, Appl. Phys. Lett. **52**, 957 (1988)
79. P. Weightman, D.S. Martin, R.J. Cole, T. Farrell, Rep. Prog. Phys. **68**, 1251 (2005)
80. T.U. Kampen, U. Rossow, M. Schumann, S. Park, D.R.T. Zahn, J. Vac. Sci. Technol. B **18**, 2077 (2000)
81. B.S. Mendoza, R. Vázquez-Nava, Phys. Rev. B **72**, 1 (2005)

http://www.springer.com/978-3-642-40127-5

Ellipsometry of Functional Organic Surfaces and Films
Hinrichs, K.; Eichhorn, K.-J. (Eds.)
2014, XXI, 363 p. 216 illus., 55 illus. in color., Hardcover
ISBN: 978-3-642-40127-5